

CHEM MED CHEM

CHEMISTRY ENABLING DRUG DISCOVERY

Accepted Article

Title: Oxadiazole Derivatives as Dual Orexin Receptor Antagonists: Synthesis, Structure-Activity-Relationship, and Sleep-Promoting Properties in the Rat

Authors: Christine Brotschi, Catherine Roch, John Gatfield, Alexander Treiber, Jodi T. Williams, Thierry Sifferlen, Bibia Heidmann, Francois Jenck, Martin H. Bolli, and Christoph Boss

This manuscript has been accepted after peer review and appears as an Accepted Article online prior to editing, proofing, and formal publication of the final Version of Record (VoR). This work is currently citable by using the Digital Object Identifier (DOI) given below. The VoR will be published online in Early View as soon as possible and may be different to this Accepted Article as a result of editing. Readers should obtain the VoR from the journal website shown below when it is published to ensure accuracy of information. The authors are responsible for the content of this Accepted Article.

To be cited as: *ChemMedChem* 10.1002/cmdc.201900242

Link to VoR: <http://dx.doi.org/10.1002/cmdc.201900242>

WILEY-VCH

www.chemmedchem.org

A Journal of



FULL PAPER

Oxadiazole Derivatives as Dual Orexin Receptor Antagonists: Synthesis, Structure-Activity-Relationship, and Sleep-Promoting Properties in the Rat.

Christine Brotschi,* Catherine Roch, John Gatfield, Alexander Treiber, Jodi T. Williams, Thierry Sifferlen, Bibia Heidmann, Francois Jenck, Martin H. Bolli, and Christoph Boss^[a]

[a] Dr. C. Brotschi, Dr. C. Roch, Dr. J. Gatfield, Dr. A. Treiber, Dr. J. T. Williams, Dr. T. Sifferlen, Dr. B. Heidmann, Dr. F. Jenck, Dr. M. H. Bolli, Dr. C. Boss.
Drug Discovery and Preclinical Research & Development
Idorsia Pharmaceuticals Ltd.
Hegenheimermattweg 91, 4123 Allschwil/BL (Switzerland)
E-mail: christine.brotschi@idorsia.com

[*] Corresponding author

Supporting information for this article is given via a link at the end of the document.

Abstract: The orexin system plays an important role in the regulation of wakefulness. Suvorexant, a dual orexin receptor antagonist (DORA) is approved for the treatment of primary insomnia. Herein, we outline our optimization efforts towards a novel DORA. We started our investigation with *rac*-[3-(5-chloro-benzooxazol-2-ylamino)-piperidin-1-yl]-(5-methyl-2-[1,2,3]triazol-2-yl-phenyl)-methanone (**3**), a structural hybrid of suvorexant and a piperidine-containing DORA. During the optimization, we resolved liabilities such as chemical instability, CYP-3A4 inhibition, and low brain penetration potential. Furthermore, structural modification of the piperidine-scaffold was essential to improve potency on the orexin 2 receptor. This work led to the identification of (5-methoxy-4-methyl-2-[1,2,3]triazol-2-yl-phenyl)-{(S)-2-[5-(2-trifluoromethoxy-phenyl)-1,2,4]oxadiazol-3-yl]-pyrrolidin-1-yl]-methanone (**51**), a potent, brain penetrating DORA with *in vivo* efficacy comparable to suvorexant in the rat.

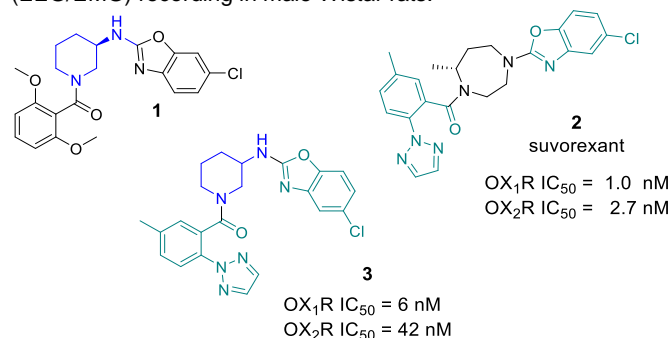
Introduction

Insomnia is a common disorder where difficulty to fall or stay asleep are the main symptoms. The cause of this phenomenon can be manifold. Until 2014, insomnia patients were predominantly treated with GABA-A potentiators, however the risk of dependence, or reduced next day performance are well described side effects emphasizing the need for further therapeutic options. In 2014, the FDA approved the first dual orexin receptor antagonist (DORA) for the treatment of insomnia under the trade name Belsontra® (suvorexant).^[1-3] The underlying mechanism of DORA's are the inhibition of orexin 1 (OX₁R) and orexin 2 receptors (OX₂R) to promote sleep by reducing wakefulness. The first proof of concept for this novel mechanism was obtained with almorexant in 2007,^[4] almost a decade after the orexin neuropeptides (orexin A and orexin B) had been discovered independently by two research groups.^[5-6] Orexins, also known as hypocretins originate from the common precursor prepro-orexin which is produced by neurons located in the hypothalamus. Orexin A binds to the G-protein-coupled receptors OX₁R and OX₂R, whereas orexin B binds mainly to OX₂R. Intense research^[7-11] resulted in the discovery of DORA's, selective orexin 1 receptor antagonists (SO₁RAs) and selective orexin 2 receptor antagonists (SO₂RAs). Almorexant was the first DORA on which clinical data were published.^[12-13] Currently, several additional DORAs (e.g., lemborexant from Eisai,^[14] compound from Idorsia^[15] and SO₂RAs (MIN-202)^[16-17] are evaluated in clinical studies for the treatment of insomnia.^[18-21] Whether blocking the

OX₂R alone is sufficient for promoting sleep in humans was under debate^[22-26] until recently when Merck published their results of MK-1064, a SO₂RA promoting sleep in mouse, dog and human in a similar manner to DORAs.^[27] SO₁RAs are investigated mainly for the treatment of addiction, stress, anxiety, and panic disorders.^[28-29] Here, we describe our efforts towards the discovery of an orally active, brain penetrating DORA, with the goal of improving OX₂R-potency of our starting point, hybrid **3**.

Results and Discussion

The following assays served to characterize and advance our compounds as well as to establish the SARs with respect to potency, safety, and efficacy. Compound potency on the orexin 1 receptor (OX₁R) and orexin 2 receptor (OX₂R) was assessed using a calcium release assay (FLIPR) where inhibition of orexin A-induced Ca²⁺ flux was determined as a functional readout of orexin receptor antagonism. Values are reported as IC₅₀ in nM and are reported as the geometric mean of at least three measurements. Earlier studies in our DORA program revealed CYP3A4 inhibition as a potential liability of our compounds and we thus systematically measured CYP3A4 inhibition using testosterone as substrate. Metabolic stability of our compounds was assessed by measuring intrinsic clearance in the presence of human liver microsomes (HLM). To assess the compound's potential to penetrate the brain, the human multidrug resistant protein transporter (MDR1) assay was used to determine the substrate susceptibility for the P-glycoprotein transporter. In addition, brain penetration was measured *in vivo* in the rat and compound concentrations in brain and plasma are expressed in ng/g and ng/mL, respectively. Finally, efficacy of our compounds was assessed using electroencephalography/ electromyography (EEG/EMG) recording in male Wistar rats.

Figure 1: Competitor compounds **1** and **2**, and our starting point hybrid **3**.

FULL PAPER

The starting point of our optimization work relied on published structures of DORAs, such as compound **1**^[30] and Merck's suvorexant (MK-4305) **2**.^[31] In house, hybrid **3**^[32] was synthesized and its racemate was determined to have an activity in the FLIPR

assay of 6 nM and 42 nM for OX₁R and OX₂R, respectively (Figure 1). The optimization route that was triggered by this promising starting point is summarized in Figure 2..

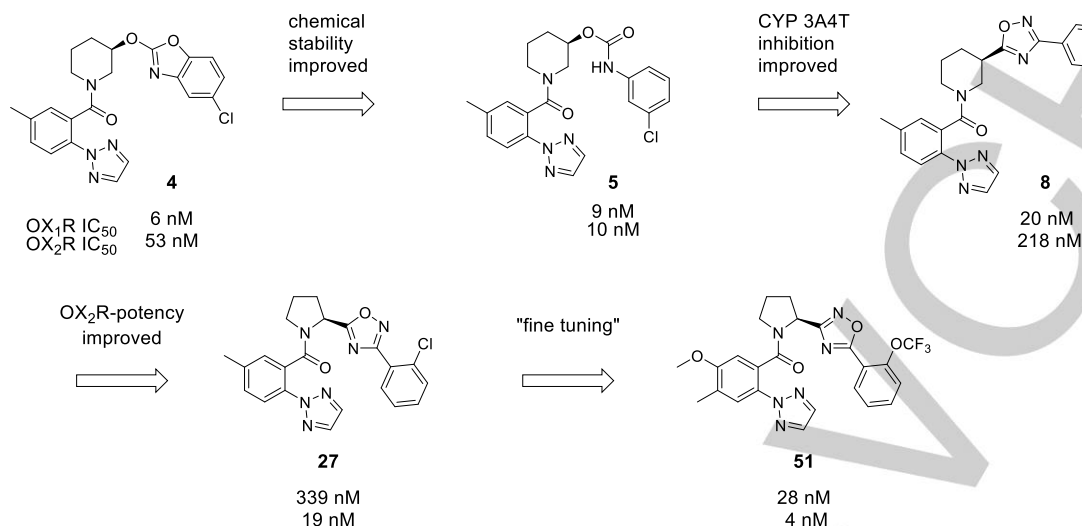


Figure 2. The optimization route via O-linked benzoxazole **4**, carbamate **5**, and oxadiazole **8** and **27**, resulted in compound **51**.

Replacing the exocyclic nitrogen-atom in **3** by an oxygen-atom in **4** had no impact on OX₁R and/or OX₂R potency, however the O-benzoxazole was chemically unstable, resulting in carbamate **5**. The carbamate analogs were equally potent, however they showed significant CYP3A4 inhibition. Converting the carbamate function into an oxadiazole moiety resolved this liability, but the OX₂R potency was diminished. Potency on OX₂R could be restored by replacing the piperidine-core by a pyrrolidine (see compound **27**). Further optimization work included the analysis of the different oxadiazole isomers and the fine tuning of the substituent on the periphery to optimize on brain penetration. The "fine tuning" also resulted in an increase in OX₁R potency.

Combining these efforts resulted in compound **51**, a highly potent, brain penetrating, and dual orexin receptor antagonist that showed efficacy in a rat EEG/EMG experiment.

In detail, a close analog of the O-linked benzoxazole-ring-analog **4** was shown to be chemically unstable under acidic conditions and hydrolyzed to the corresponding carbamate. Interestingly, carbamate **5** was similar in potency to its benzoxazole analog **4**. Changing the substitution pattern to 2,5-dimethyl (**6**) increased potency on OX₂R, when compared to **5**, and 3,5-dimethyl analog **7** showed potencies of 2 nM on both OXRs (Table 1).

Table 1. Carbamates vs. Oxadiazoles.

		Carbamate			Oxadiazole				
R	Cpd	OX ₁ R ^[a]	OX ₂ R ^[a]	CYP3A4 ^[b]	Cpd	OX ₁ R ^[a]	OX ₂ R ^[a]	CYP3A4 ^[b]	
	5	6	19	6	8	48	239	34	
	6	21	6	4	9	13	60	28	
	7	2	2	5	10	1.5	27	24	

[a] IC₅₀ in nM. Values are the geometric mean (± 2-fold) of at least three independent experiments and were determined by FLIPR assay (see Supporting Information for assay details); [b] IC₅₀ in μM, values are from single measurements with testosterone used as substrate; nd = not determined.

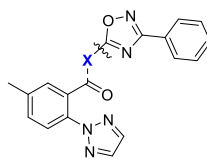
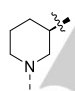
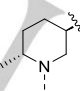
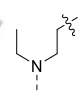
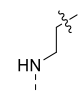
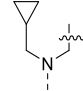
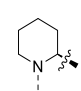
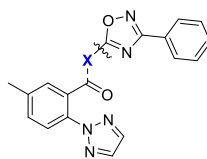
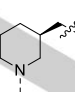
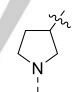
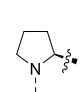
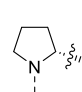
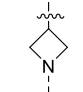
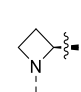
FULL PAPER

Unfortunately, carbamates **5**, **6**, and **7** showed inhibitory activity towards CYP3A4 in the range of 3 to 6 μM . Furthermore, all carbamates tested *in vivo* for brain penetration in rat (measured 3 h after oral dosing of 100 mg/kg) showed low plasma and brain concentrations. The most potent compound **7** had plasma and brain concentrations of 189 ng/mL and 49 ng/g, respectively. Our task therefore was to replace the carbamate moiety to alter the overall physicochemical properties to reduce CYP3A4 inhibition and to increase plasma and brain concentrations, without diminishing OX₂R potency.

Our attempt to replace the carbamate moiety by an oxadiazole was encouraging. The antagonistic activity of the oxadiazole derivative **8** showed a profile with a 5-fold preference for OX₁R (48 nM and 239 nM on OX₁R and OX₂R, respectively) and the CYP 3A4 inhibition of compound **8** was markedly reduced with an IC₅₀ value of 34 μM compared to 6 μM for **5**. The oxadiazole analogs **9** and **10** showed as well weaker CYP 3A4 inhibition when compared to their carbamate analogs (see **9** vs. **6** and **10** vs. **7**). However, no oxadiazole analog reached sufficient potency on the OX₂R. Furthermore, plasma and brain concentrations (3 h after oral dosing of 100 mg/kg to rats) of **10** (45 ng/mL and 81 ng/g, respectively) were as low as for carbamate analog **7**. In contrast to SAR investigations performed by Merck,^[33] substituent alterations on the peripheral part such as on the oxadiazole-moiety as well as on the biaryl-carboxamide-motif in our hands did not lead to the desired increase in potency on OX₂R. Furthermore, Merck published on 5-oxazole-2-methyl-piperidine^[34] and 5-thiazole-2-methyl-piperidine analogs^[35] with profiles ranging from dual to OX₂R selective antagonists.

We turned our attention to modifying the core, since we knew from in house data, that core modifications can influence the selectivity profile of a class of compounds.^[36] For our SAR studies, we kept the aryl-triazolyl-carboxamide and the unsubstituted phenyl-oxadiazole constant, and investigated the impact of replacing the piperidine-core on potency and selectivity (see Table 2). Ideally, the core-replacement would lead to compounds with increased potency on OX₂R and therefore to compounds with a DORA profile. Introduction of a methyl-group at the 6-position of the piperidine-ring (trans-racemate **12**) improved the potency on both receptors equally. Interestingly, the less constrained compound **13** was more potent on both OXRs when compared to piperidine-analog **11**. The selectivity profile of the ring opened analog **13** was even more OX₁R preferential than **11** (20-fold) and therefore of no interest to us. Analog **14** showed a major drop in potency, indicating that a tertiary carboxamide is preferred. When the linker was shortened by one C-atom (**15**) the potency on both OXRs was reduced dramatically. Compound **16**, with an exit vector shifted to position C-2, resulted in a potency loss of more than 10-fold on both receptors when compared to **11**. Similarly, when the exit vector was kept at C-3 but elongated by one C-atom (**17**), a drop in potency was observed. The potency of the 3-pyrrolidine (**18**) and the 3-azetidine (**21**) was also markedly reduced. On the other hand, the 2-substituted pyrrolidine (**19**) and azetidine derivative (**22**) were identified as DORA's with preference for OX₂R (6-fold and 16-fold, respectively). Besides potency, we were also interested in core modifications that led to metabolically more stable compounds in HLM when compared to those containing the piperidine core.

Table 2: Core-replacements

							
	Cpd	11	12 trans-rac	13	14	15	16
	OX ₁ R ^[a]	40	6	4	1005	2758	640
	OX ₂ R ^[a]	334	66	85	2463	690	3510
	HLM ^[b]	85	153	177	nd	nd	nd
							
	Cpd	17	18	19	20	21	22
	OX ₁ R ^[a]	1128	1113	486	3167	2117	4150
	OX ₂ R ^[a]	652	1021	76	2887	3883	262
	HLM ^[b]	nd	nd	50	nd	nd	19

[a] IC₅₀ in nM. Values are the geometric mean (\pm 2-fold) of at least three independent experiments and were determined by FLIPR assay (see Supporting Information for assay details); [b] Intrinsic metabolic clearance [$\mu\text{L min}^{-1} \text{mg}^{-1}$] with human liver microsomes, at 1 μM ; nd = not determined

Overall, compound **19** was the most potent compound on OX₂R and, compared to other core modifications, its rather low intrinsic clearance of 50 $\mu\text{L min}^{-1} \text{mg}^{-1}$ in HLM, made the pyrrolidine the most attractive core-replacement for further SAR studies. The R-enantiomer **20** was substantially less potent on both receptors, therefore the following SAR was performed on the more potent S-

enantiomer only. We also performed optimization work on azetidine-analogs. These efforts resulted in potent OX₂R preferential compounds, but none of the azetidine analogs tested *in vivo* reached reasonable plasma and brain concentrations (data not shown).

FULL PAPER

Table 3: SAR studies of oxadiazole-pyrrolidine-analogs with different R moieties

R							
Cpd	19	23	24	25	26	27	28
OX ₁ R ^[a]	486	128	352	1034	64	339	72
OX ₂ R ^[a]	76	16	36	194	37	19	9

R							
Cpd	29	30	31	32	33	34	35
OX ₁ R ^[a]	123	40	13	92	92	22	22
OX ₂ R ^[a]	8	7	8	11	19	4	7
MDR1 efflux ^[b]	1.3	1.3	2.2	nd	nd	nd	2.5
Papp A-B ^[c]	24.5	36.3	30.7	nd	nd	nd	17.8

[a] IC₅₀ in nM. Values are the geometric mean (± 2-fold) of at least three independent experiments and were determined by FLIPR assay (see Supporting Information for assay details); [b] multidrug resistance protein 1 (MDR1) efflux ratio (Papp B-A/Papp A-B); [c] passive permeability Papp A-B (10⁻⁶ cm s⁻¹); nd = not determined.

In a next step, the R moiety attached to the oxadiazole and its substitution pattern were investigated (Table 3). A 2-methyl (**23**), a 2-methoxy (**26**) and a 2-chloro substituent (**27**) showed improved potency compared to the unsubstituted analog **19**. A 2-methyl substituent (**23**) was preferred when compared to a 3-methyl (**24**), and a 4-methyl group was substantially less potent (**25**). A 2-trifluoromethoxy-substituent (**31**) led to the most potent mono-substituted compound on both OX₁R and OX₂R. A di-substituted compound with a 2-chloro, 3-methyl substitution (**29**) improved potency in comparison to mono-substituted **27**. Its 2-methyl-3-chloro isomer **30** showed similar OX₂R potency and a threefold improved OX₁R potency. The 2-methoxy-3-fluoro substitution (**28**) showed an improved potency on OX₂R when compared to mono-substituted **26**. Additional substitution patterns such as 2,5-dimethyl (**32**) or 3,5-dimethyl (**33**) improved potency on both OXRs indicating that a variety of modifications are tolerated by the receptors. Compound **33** showed that an ortho substituent is not mandatory, however, for most analogs an ortho substituent was beneficial. Increasing the length of the substituent to 2-ethoxy (**34**) improved the potency further (threefold on OX₁R and 9-fold on OX₂R) when compared to 2-methoxy (**26**). The more polar pyridine analog **35** was tolerated by both OXRs, showing similar potency when compared to phenyl analog **34**. A few analogs were tested in a permeability assay containing the human multidrug resistance protein 1 (MDR1, P-gp) to evaluate transmembrane permeability and P-gp substrate potential. A MDR1 efflux ratio of 1.3 to 2.5 indicated that these compounds are not, or weak substrates of the MDR1 efflux pump. The Papp(A-B) values were in the range of 18 - 36 x 10⁻⁶ cm s⁻¹ suggesting that all compounds are highly permeable.

In an attempt to reduce lipophilicity, heterocycles replacing the R-phenyl ring were investigated (Table 3). Pyridine analog **35** showed high affinity for both OXRs and represents a compound with higher brain free fraction when compared to the phenyl analogs **29** to **31**.

Next, we explored the SAR of the *o*-biaryl benzamide, keeping the (S)-5-(pyrrolidin-2-yl)-3-(2-(trifluoromethoxy) phenyl)-1,2,4-oxadiazole scaffold constant (Table 4).

Table 4: Optimization of the biaryl carboxamide of oxadiazole-pyrrolidine-analogs

R					
Cpd	36	31	37	38	39
OX ₁ R ^[a]	59	13	47	31	56
OX ₂ R ^[a]	29	8	34	15	18
HLM ^[b]	187	170	89	266	189

R					
Cpd	40	41	42	43	44
OX ₁ R ^[a]	65	37	364	33	5
OX ₂ R ^[a]	18	4	72	24	5
HLM ^[b]	nd	424	72	nd	335

[a] IC₅₀ in nM. Values are the geometric mean (± 2-fold) of at least three independent experiments and were determined by FLIPR assay (see Supporting Information for assay details); [b] Intrinsic metabolic clearance [μL min⁻¹ mg⁻¹] with human liver microsomes, at 1 μM; nd = not determined

FULL PAPER

In comparison to **31**, the unsubstituted triazolyl benzamide **36** and the 5-chloro analog **37** were weaker in affinity at both OXRs. Shifting the substituent from position 5 to position 4 was tolerated in the case of **38** and **39**. Replacing the triazole by a pyrimidine (**40**) led to a loss in potency on both OXRs. All di-substituted benzamides had a higher OX₂R affinity than their mono-substituted analogs, see **41** and **44**. In addition to the potency, human microsomal stability was measured. We observed that the di-substituted analogs had lower microsomal stability than the mono-substituted analogs. Metabolite identification studies revealed that the methyl at the 4 position of the 4-methyl-5-methoxybenzamide was metabolically labile (data not shown), therefore we replaced this metabolic hotspot by a fluorine and indeed, **42** showed an improved stability in HLM ($CL_{int} = 72 \mu\text{L min}^{-1} \text{mg}^{-1}$ compared to $424 \mu\text{L min}^{-1} \text{mg}^{-1}$ for **41**). Unfortunately, this modification resulted in an unacceptable drop in potency on both OXRs.

Next, we investigated the various oxadiazole-isomers with respect to their impact on potency and microsomal stability (see Table 5). Asymmetric 1,2,4-oxadiazoles **31** (isomer A) and **45** (isomer B) were similar in potency, whereas the symmetric 1,3,4-oxadiazole analog **46** (isomer C) showed a reduced potency on both OXRs, indicating that the position of the heteroatoms (dipole moment) does play a role for receptor binding affinity.^[37] Oxadiazole isomer C (**46**) was slightly more stable than isomers A and B ($CL_{int} = 96$ vs. 170 and 148 $\mu\text{L min}^{-1} \text{mg}^{-1}$ for **31** and **45**) in HLM. The slight improvement in *in vitro* stability was in line with reported data for symmetric oxadiazole analogs compared to the NO-bond comprising asymmetric oxadiazoles.^[38]

Table 5. Oxadiazole isomers A, B, and C

Cpd	X		
	isomer A	isomer B	isomer C
OX ₁ R ^[a]	13	14	184
OX ₂ R ^[a]	8	4	118
HLM ^[b]	170	148	96

[a] IC₅₀ in nM. Values are the geometric mean (\pm 2-fold) of at least three independent experiments and were determined by FLIPR assay (see Supporting Information for assay details); [b] Intrinsic metabolic clearance [$\mu\text{L min}^{-1} \text{mg}^{-1}$] with human liver microsomes, at 1 μM .

The potency loss on the OXRs caused by the symmetrical oxadiazole C could be compensated by introducing a disubstituted ortho-triazolyl benzamide (e.g. **49**, Table 6). Unfortunately, compound **49** (isomer C) was less stable in HLM than **47** or **48** (isomer A or B) suggesting that peripheral substituents influence the microsomal clearance of the compounds to a greater extent than the arrangement of the atoms in the oxadiazole ring.

To assess whether our compounds penetrate into brain tissue, a series of *in vivo* experiments were performed in male Wistar rats. Absolute brain- and plasma concentrations were determined 3 h after oral dosing (100 mg/kg) and the results of a selection of compounds are summarized in Table 6.

Table 6. Oxadiazole isomers A, B, and C

SF ^[a]	Cpd	Isomer	X	OX ₁ R ^[b]	OX ₂ R ^[b]	HLM ^[c]	[P] ^[d]	[B] ^[d]	[B/P] ^[e]	[CSF] ^[f]	MDR1 efflux ^[g]
	47	A		13	3	192	309	483	1.56	5.2	1.4
	48	B		7	1	258	893	351	0.39	2.1	nd
	49	C		30	5	364	121	96	0.79	3	nd
	35	A		22	7	71	140	53	0.38	4.7	2.5
	50	B		5	2	151	259	165	0.64	17.4	6.2
	41	A		37	4	424	2237	3253	1.45	31.5	1.8
	51	B		28	4	282	1763	1585	1.62	19.8	2.1

[a] SF = scaffold; [b] IC₅₀ in nM. Values are the geometric mean (\pm 2-fold) of at least three independent experiments and were determined by FLIPR assay (see Supporting Information for assay details); [c] Intrinsic metabolic clearance [$\mu\text{L min}^{-1} \text{mg}^{-1}$] with human liver microsomes, at 1 μM ; [d] brain penetration experiment was performed in rat (n=3) by sampling plasma and brain, 3 h following administration of 100 mg/kg po; [e] brain/plasma ratios were calculated assuming a brain density around 1 g/mL; [f] CSF = cerebral spinal fluid [ng/mL]; [g] multidrug resistant protein 1 (MDR1) efflux ratio of (Papp B-A/Papp A-B); nd = not determined.

FULL PAPER

By comparing plasma and brain concentrations of oxadiazole-isomer A with those of isomer B, we could not find a trend for increased concentrations for one of the two isomers (comparison of **47** with **48**, **35** with **50**, and **41** with **51**). However, the symmetrical [1,3,4]-oxadiazole isomer C (see **49**) showed lower concentrations in plasma and brain when compared to the asymmetrical oxadiazole analogs (**47**, **48**). Compounds **35** and **50**, both bearing a 2-ethoxypyridine, exhibited low plasma and brain concentrations. Plasma and brain concentrations of pyridine analogs appeared to be inferior to the more lipophilic analogs either due to lower absorption and/or due to a higher efflux by P-gp (see **50**). Of all compounds investigated, **41**, **47**, and **51** reached the highest plasma and, in particular, brain concentrations in the rat. These compounds were tested for their human MDR1 susceptibility and their efflux ratios were in an acceptable range between 1.4 and 2.5, confirming earlier measurements suggesting that these compounds are not substrates of the human MDR1 transporter protein and are therefore viable candidates for further characterization.

We thus chose to advance **41**, **47** and **51** and to test them *in vivo* for their effect on the sleep/wake stages. We used freely moving male Wistar rats implanted with radiotelemetric transmitters for continuous recording of EEG/EMG signals. In a first step, **41**, **47**, and **51** were tested at 100 mg/kg po administered at the beginning of the nocturnal active phase, when endogenous orexin levels increase. Over the 12 h night period following administration, compound **51** showed a similar sleep promoting effect as suvorexant when tested under the same experimental conditions (Figure 3). Compared to vehicle treated rats, **51** significantly decreased the time spent in active wake (-24% and -17% vs. matched vehicle for **51** and suvorexant, respectively; $p < 0.001$ for **51** and suvorexant, paired t-test), and significantly increased both the time spent in non-REM (rapid eye movement) sleep (+14.3% and +21.6% for **51** and suvorexant, respectively; $p < 0.001$ for **51** and suvorexant, paired t-test) and the time spent in REM sleep (+35.2% and +21.6% for **51** and suvorexant; respectively; $p < 0.05$ for **51** and not statistically significant for suvorexant with $p = 0.0714$, paired t-test). As is usually observed with DORAs,^[31, 39-45]

the relative proportion of the time spent in non-REM and REM sleep over the total sleep time remained unchanged (~82 % and ~18%, respectively for all groups, compared to matched-vehicle treated rats; $p = 0.1697$ for **51** and $p = 0.7385$ for suvorexant, paired t-test). Under the same conditions (Figure 3), compounds **41** and **47** showed a less pronounced sleep promoting effect compared to compound **51**. Both decreased significantly the time spent in active wake compared to vehicle treated rats (-13.9% and -7.3% vs. vehicle for **41** and **47**; respectively; $p < 0.05$ for **41** and **47**). However, a significant increase was only observed for the time spent in non-REM sleep (+7.3% ($p < 0.05$) and +11.2% ($p < 0.01$) vs. vehicle for **41** and **47**, respectively). The time spent in REM sleep was marginally increased compared to vehicle treated rats (+0.9% ($p = 0.7403$) and +7.8% ($p = 0.2570$) vs. vehicle for **41** and **47**, respectively). In contrast to compound **47**, compound **41** significantly increased the time spent in quiet wake compared to vehicle treated rats (+19.2 % vs. vehicle, $p < 0.05$). For both, the relative proportion of the time spent in non-REM and REM sleep over the total sleep time remained unchanged (~82% non-REM sleep and ~18% REM sleep for **41** and matched vehicle treated group ($p = 0.0549$) and ~85% non-REM sleep and ~15% REM sleep for **47** and matched vehicle treated group ($p = 0.8272$)). Due to its promising sleep promoting effect at 100 mg/kg and to fully evaluate the potential of **51**, we tested **51** at a lower dose of 30 mg/kg. At this dose, over the 12 h night period following administration, **51** still significantly decreased the time spent in active wake (-9.7% vs. vehicle, $p < 0.05$) and increased the time spent in non-REM sleep (+8% vs. vehicle, $p < 0.05$). The increase of the time spent in REM sleep was no longer significant (+11% vs. vehicle, $p = 0.1084$). In this experiment, compound **51** increased slightly but significantly the time spent in quiet wake compared to vehicle treated rats (+8.3% vs. vehicle, $p < 0.05$). The same pattern of pharmacological activity was observed with suvorexant at 30 mg/kg (-8.7% vs. vehicle ($p < 0.05$) for the time spent in active wake, +12.5% vs. vehicle ($p < 0.001$) for the time spent in non-REM sleep, and +11.1% ($p = 0.0815$) for the time spent in REM sleep.

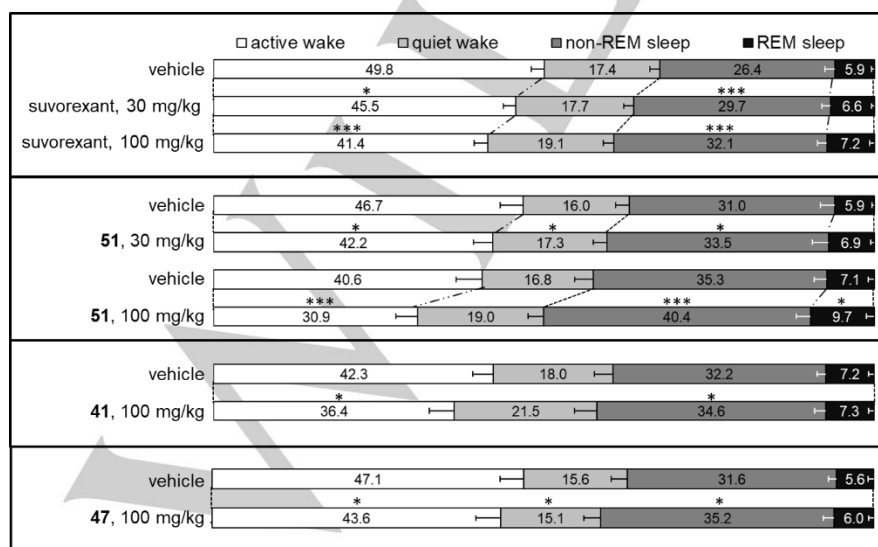


Figure 3. Effect of suvorexant, **51**, **41**, and **47** on the time spent in sleep and wake stages (% of total time) during the 12 h night active period post administration in male Wistar rats. Rats were administered a single oral dose of vehicle (PEG 400) or compound. Data are expressed as mean \pm SEM. * $p < 0.05$, ** $p < 0.01$, *** $p < 0.001$ ($n = 14$ for suvorexant, $n = 8$ for **51**, **41**, and **47**).

FULL PAPER

Table 7. IC₅₀ and K_i values at human, rat, and dog orexin receptors.

Cpd	IC ₅₀ ^[a] hOX ₁ R	IC ₅₀ ^[a] hOX ₂ R	K _i ^[b] hOX ₁ R	K _i ^[b] hOX ₂ R	K _i ^[b] rOX ₁ R	K _i ^[b] rOX ₂ R	K _i ^[b] dOX ₁ R	K _i ^[b] dOX ₂ R
47	13	2	6.8	2.4	14	1.6	4.7	1.1
41	29	3	13	1.0	11	1.6	32	1.6
51	27	3	17	1.3	10	1.3	9	1.1

[a] IC₅₀ in nM. Values are the geometric mean (± 2-fold) of at least three independent experiments and were determined by FLIPR assay (see Supporting Information for assay details); [b] K_i values are in nM and calculated via the Cheng-Prusoff equation from single FLIPR experiments run in duplicates.

Orexin receptors are conserved across species and compounds were assessed in human, rat, and dog K_i measurements and shown to be equipotent across species (Table 7).

For all compounds measured, CL_{int} in rat liver microsomes (RLM) was above 1250 μL min⁻¹ mg⁻¹. We therefore performed brain penetration experiments and *in vivo* EEG-experiments in rats at the high dose of 100 mg/kg with the intention of saturating metabolic processes. To further evaluate the potential of compound **51**, we assessed pharmacokinetic properties at lower doses where less or no saturation was expected. To evaluate

potential species differences, we compared the pharmacokinetic profiles in the rat and the dog (Table 8). Compound **51** showed plasma clearance of 96 mL min⁻¹ kg⁻¹ in the rat, and of 17 mL min⁻¹ kg⁻¹ in the dog. Considering blood-to-plasma partitioning and the respective liver blood flows; compound **51** was classified as a high clearance compound in the rat and a moderate-to-high clearance compound in the dog. This correlated with the observed differences in intrinsic clearance in dog liver microsomes (DLM) (CL_{int} = 543 μL min⁻¹ mg⁻¹) when compared to RLM (CL_{int} >1250 μL min⁻¹ mg⁻¹).

Table 8. Pharmacokinetics of **51** in rat and dog

Species	iv ^[a]				po ^[b]				
	Dose [mg kg ⁻¹]	CL [mL min ⁻¹ kg ⁻¹]	V _{ss} [L kg ⁻¹]	T _{1/2} [h]	Dose [mg kg ⁻¹]	AUC [ng h mL ⁻¹]	C _{max} [ng mL ⁻¹]	T _{max} [h]	F [%]
rat	0.1	96	1.2	0.2	10 ^[c]	168	69.8	1	10
dog	0.1	17	1.3	1.3	2.2 ^[d]	896	576	0.5	43

[a] iv = intravenous, formulation: HPβCD/DMSO 95%/ 5% in 30% H₂O; [b] oral; [c] formulation: 0.5% methylcellulose (MC); [d] formulation: Cremophor RH40/Lauroglycol 90; HPβCD = Hydroxypropyl Beta Cyclodextrin.

As volume of distribution was similar between both species, the difference in clearance translated into a shorter half-life of 0.2 h in rat compared to 1.3 h in the dog. Also, the bioavailability in dog was higher compared to rat, i.e. 43 % vs. 10 %, respectively. With this encouraging data in hand further profiling was performed and the data are summarized in Table 9. Compound **51** showed no relevant competitive or time-dependent inhibition of CYP3A4, CYP2D6, and CYP2C9, no formation of reactive metabolites in a glutathione trapping assay, and no inhibition of the hERG channel was observed at the highest concentration measured (IC₅₀ >20 μM).

Table 9. Profile of **51**

	IC ₅₀ [μM]	time dependent inhibition (IC ₅₀ shift assay)
P450 inhibition	CYP3A4	8.1
	CYP2D6	29
	CYP2C9	3
dGSH Trapping [pmol mg ⁻¹ h ⁻¹]	<100	
hERG	>20	

In a panel of 50 ion channel, receptor and transporter assays, compound **47** showed interactions with the serotonin 5-HT_{2B} receptor (IC₅₀ of 0.67 μM) and the dopamine transporter (DAT,

IC₅₀ of 0.34 μM). For compound **51** no significant inhibitory activities were detected for these two off-targets (IC₅₀ of 16 μM and greater than 30 μM on serotonin 5-HT_{2B} and DAT, respectively).

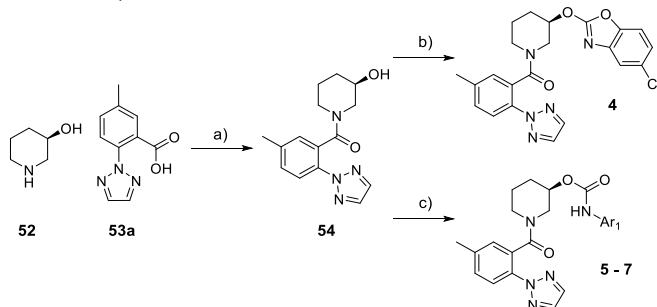
In summary, our structural optimization started with hybrid **3**, the instability of the ether-linked analog **4** resulted in carbamate analogs which revealed inhibitory activities on CYP 3A4. Converting the carbamate function into an oxadiazole moiety resolved this liability, however OX₂R potency was diminished. Changing the core structure from a piperidine to a pyrrolidine restored potency on the OX₂R and resulted in the discovery of a novel pyrrolidine-oxadiazole series. Among these compounds, the 1,2,4-oxadiazole **51** was found to be a potent, orally available, brain penetrating dual orexin receptor antagonist, which showed sleep-promoting effects comparable to suvorexant in rats.

Chemistry

The synthesis^[46] of compounds **4** to **51** are summarized in Schemes 1-6. The oxygen linked benzoxazole **4** was prepared starting from commercially available (*R*)-3-hydroxypiperidine HCl (**52**) (Scheme 1). Amide coupling of **52** and **53a**^[31-32] afforded intermediate **54**, which upon nucleophilic substitution with 2,5-dichlorobenzo[d]oxazole, yielded **4**. Carbamate **5** was prepared from **54** and commercially available 3-chlorophenyl isocyanate

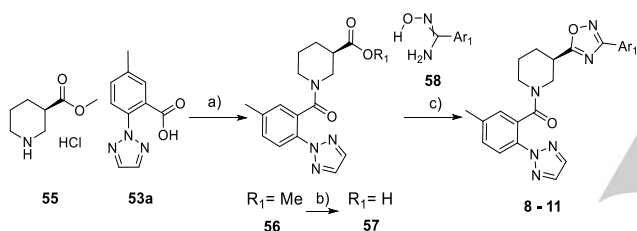
FULL PAPER

under basic conditions. Compounds **6** and **7** were synthesized accordingly, using the corresponding isocyanates (see supporting information).



Scheme 1: Synthesis of O-linked benzoxazole **4** and carbamates **5-7**. Reagents and conditions: a) TBTU, DIPEA, DCM, rt, 3 h; b) (i) NaH, THF, rt, 30 min; (ii) 2,5-dichlorobenzo[d]oxazole, THF, rt, 18 h; c) (i) NaH, THF, 0 °C to rt, 20 min; (ii) corresponding isocyanate, THF, rt, 2.5 h.

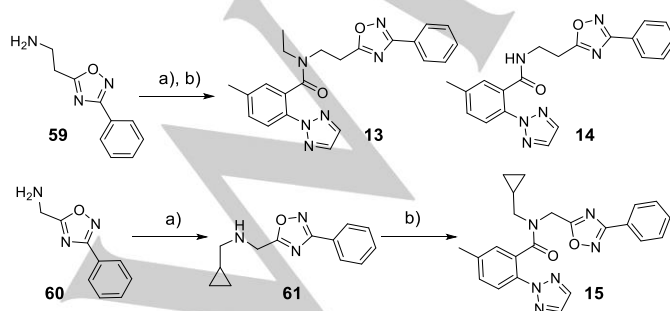
Compounds containing a cyclic core structure (**8** to **11**, **12**, **16-22**) were synthesized in analogy to Scheme 2, using corresponding starting materials. For simplicity, only piperidine analogs are outlined in Scheme 2.



Scheme 2: Synthesis of oxadiazole-piperidine analogs. Reagents and conditions: a) TBTU, DIPEA, DCM, rt, 18 h; b) 2 N aq. NaOH, EtOH/THF, rt, 1.5 h; c) (i) PyBOP, DIPEA, DCM, rt, 16 h; (ii) dioxane, 90 °C, 16 h.

Compound **8** to **11** were synthesized starting from commercially available methyl (*R*)-piperidine-3-carboxylate HCl **55**, which upon amide coupling with **53a** yielded intermediate **56**. Saponification of the ester function under basic conditions yielded carboxylic acid **57**, which was converted to oxadiazoles in a two-step procedure; amide coupling with corresponding hydroxyamidine **58**, followed by thermal cyclization.

The synthesis of ring opened-analogs **13** to **15** is outlined in Scheme 3. Commercially available amines **59** and **60** were submitted to reductive amination conditions followed by amide coupling.

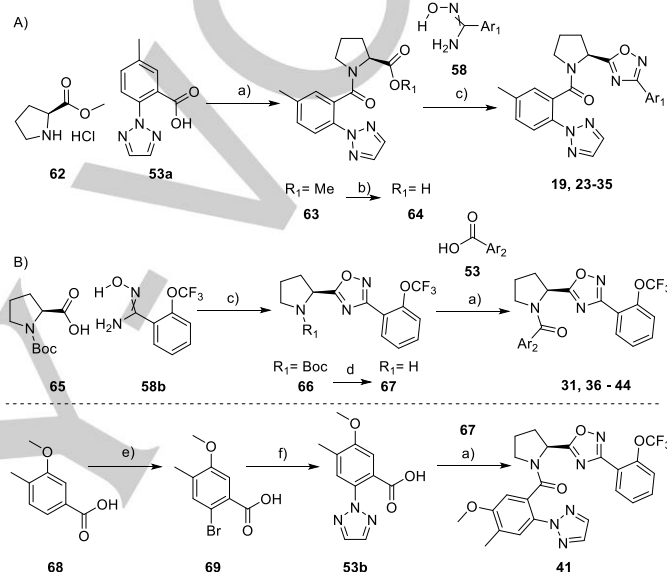


Scheme 3: Synthesis of oxadiazole-analogs with open form core-structures. Reagents and conditions: a) corresponding aldehyde (acetaldehyde or

cylcolpropylcarboxaldehyde), TEA, MeOH, NaBH₄, rt, 18 h; b) **53a**, TBTU, DIPEA, DMF, rt, 18 h.

The pyrrolidine-oxadiazole analogs of isomer A (**19**, **23-25**, **31**, and **36-44**) were synthesized via one of the two approaches outlined in Scheme 4, approach A or B.

For Approach A, commercially available L-proline methyl ester HCl (**62**) was coupled with **53a** in an amide coupling to intermediate **63**. After ester hydrolysis under basic conditions, carboxylic acid **64** and corresponding hydroxyamidine **58** were coupled, followed by thermal cyclization to yield compounds **19** and **23-35**. The substituted hydroxyamidines **58** were either commercially available or synthesized from the corresponding carboxylic acid (see supporting information).



Scheme 4: General synthesis of pyrrolidine-oxadiazole analogs of isomer A, and compound **41** as a specific example. Reagents and conditions: a) TBTU, DIPEA, DCM, rt, 18 h; b) 2 N aq. NaOH, EtOH/THF, rt, 1.5 h; c) (i) PyBOP, DIPEA, DCM, rt, 16 h; (ii) dioxane, 90 °C, 16 h; d) TFA, DCM, 0 °C to rt, 5 h; e) Br₂, acetic acid/H₂O, 60 °C, 2 h; f) CuI, DMEDA, Cs₂CO₃, 1*H*-1,2,3-triazole, DMF, 120 °C, 1 h.

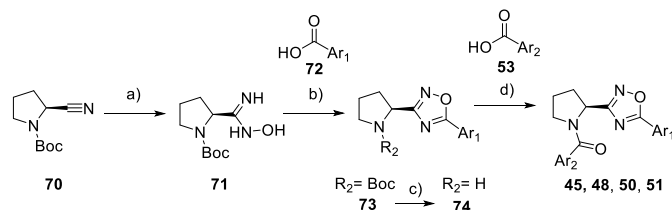
For Approach B, commercially available (*tert*-butoxycarbonyl)-L-proline (**65**) and hydroxyamidine **58a** were converted in a two-step procedure into intermediate **66**, boc-deprotection with TFA, followed by amide coupling of **67** and ortho-biaryl carboxylic acid **53**, led to compound **31** and **36-44**. The synthesis of compound **41** is outlined as a representative for compounds **36** to **44**, following Approach B.

The synthesis of the *ortho*-biaryl carboxylic acid **53b** was synthesized from commercially available benzoic acid **68**. Selective bromination with Br₂ in acetic acid/H₂O mixture led to compound **69**, which was converted via a copper mediated coupling reaction to **53b**. Amide coupling of **53b** and amine **67** yielded compound **41**. Syntheses of other biaryl acids **53** are described in the literature^[46] or in the supporting information.

The pyrrolidine-oxadiazole analogs of isomer B were synthesized according to Scheme 5. Commercially available boc-protected nitrile **70** was converted to the hydroxyamidine **71**. Amide coupling with the corresponding carboxylic acid **72**, followed by thermal cyclization yielded **73**. Boc-deprotection yielded the

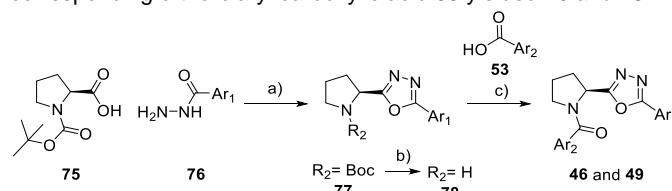
FULL PAPER

corresponding amine **74** which was converted via amide coupling to final compounds **45**, **48**, **50**, and **51**.



Scheme 5: Synthesis of oxadiazoles, isomer B. Reagents and conditions: a) hydroxylamine HCl, Na₂CO₃, MeOH, 70 °C, 1 h; b) (i) TBTU, DIPEA, DCM, rt, 1.5 h; (ii) dioxane 80 °C, 2 d; c) TFA, DCM, rt, 1.5 h; d) corresponding **53**, TBTU, DIPEA, DCM, rt, 1.5 h.

The synthesis of symmetrical oxadiazoles **46** and **49** is outlined in Scheme 6. Commercially available **75** and **76** were converted to intermediate **77** in a two-step procedure. First, coupling of hydrazine **76**, followed by cyclization in the presence of the Burgess reagent at elevated temperature resulted in **77**. After boc-deprotection with TFA, amide coupling of amine **78** with the corresponding ortho-biaryl carboxylic acid **53** yielded **46** and **49**.



Scheme 6: Synthesis of symmetrical oxadiazole analog **46** and **49**. Reagents and conditions: a) (i) PyBOP, DIPEA, DCM, rt, 16 h; (ii) Burgess reagent, dioxane, microwave irradiation, 110 °C, 30 min; b) TFA, DCM, rt, 16 h; c) TBTU, DIPEA, DMF, rt, 18 h.

Experimental Section

Commercially available starting materials were used as received without further purification. All reactions were carried out under an atmosphere of nitrogen or argon. Compounds were purified by flash chromatography on silica gel, or by preparative HPLC. Compounds described below are characterized by LC-MS data (retention time *t_R* is given in min, molecular weight obtained from the mass spectrum is given in g/mol using the conditions below. In cases where compounds appeared as a mixture of conformational isomers, as visible in their LC-MS spectra, the retention time of the most abundant conformer was given.

Mass spectrometry data were recorded by one of the following methods:

LC-MS with acidic conditions

Method A: Agilent 1100 series with mass spectrometry detection (MS: Finnigan single quadrupole). Column: Zorbax SB-aq (3.5 μm, 4.6 x 50 mm). Conditions: MeCN [eluent A]; H₂O + 0.04% TFA [eluent B]. Gradient: 95% B → 5% B over 1.5 min (flow: 4.5 mL/min). Detection: UV/Vis + MS.

Method B: Agilent 1100 series with mass spectrometry detection (MS: Finnigan single quadrupole). Column: Waters XBridge C18 (2.5 μm, 4.6 x 30 mm). Conditions: MeCN [eluent A]; H₂O + 0.04% TFA [eluent B]. Gradient: 95% B → 5% B over 1.5 min (flow: 4.5 mL/min). Detection: UV/Vis + MS.

LC-MS with basic conditions

Method C: Agilent 1100 series with mass spectrometry detection (MS: Finnigan single quadrupole). Column: Waters XBridge C18 (5 μm, 4.6 x 50 mm).

Conditions: MeCN [eluent A]; 13 mmol/L NH₃ in H₂O [eluent B]. Gradient: 95% B → 5% B over 1.5 min (flow: 4.5 mL/min). Detection: UV/Vis + MS.

LC-HRMS parameters were the following: analytical pump Waters Acquity binary, Solvent Manager, MS, SYNAPT G2 MS, source temperature of 150 °C, desolvation temperature of 400 °C, desolvation gas flow of 400 L/h; cone gas flow of 10 L/h, extraction cone of 4 RF; lens 0.1 V; sampling cone 30; capillary 1.5 kV; high resolution mode; gain of 1.0, MS function of 0.2 s per scan, 120–1000 amu in full scan, centroid mode. Lock spray: keucine enkephalin, 2 ng/mL (556.2771 Da), scan time of 0.2 s with interval of 10 s and average of 5 scans; DAD: Acquity UPLC PDA detector. Column was an Acquity UPLC BEH C18 1.7 μm, 2.1 mm x 50 mm from Waters, thermostated in the Acquity UPLC column manager at 60 °C. Eluents were the following: H₂O + 0.05% formic acid; B, acetonitrile + 0.05% formic acid. Gradient was 2% to 98% B over 3.0 min. Flow was 0.6 mL/min. Detection was at UV 214 nm. In cases where final compounds appear as a mixture of conformational isomers, visible in their LC-MS spectra, the retention time of the most abundant conformer is given.

Preparative HPLC with acidic conditions

Method D: Column: Waters XBridge (10 μm, 75 x 30 mm). Conditions: MeCN [eluent A]; H₂O + 0.5% HCOOH [eluent B]; Gradient: 90% B → 5% B over 6.4 min (flow: 75 mL/min). Detection: UV/Vis + MS.

Method E: Column: Waters Atlantis (10 μm, 75 x 30 mm). Conditions: MeCN [eluent A]; H₂O + 0.5% HCOOH [eluent B]; Gradient: 90% B → 5% B over 6.4 min (flow: 75 mL/min). Detection: UV/Vis + MS.

Preparative HPLC with basic conditions

Method F: Column: Waters XBridge (10 μm, 75 x 30 mm). Conditions: MeCN [eluent A]; H₂O + 0.5% NH₄OH (25% aq.) [eluent B]; Gradient: 90% B → 5% B over 6.5 min (flow: 75 mL/min). Detection: UV/Vis + MS

Flash column chromatography (FC) was performed either conventional or by using Biotage SNAP cartridges (10–340 g) and elution was with a Biotage Isolera system. Merck pre-coated thin layer chromatography (TLC) plates were used for TLC analysis.

¹H NMR and ¹³C NMR spectra were recorded on a Bruker (400 or 500 MHz) spectrometer in the indicated deuterated solvent. Chemical shifts are reported in ppm relative to solvent peaks as the internal reference. Due to hindered rotation, our compounds exist in multiple conformations on the NMR time-scale, similar to the diazepane series reported by Merck^[31], therefore ¹H NMR and ¹³C NMR spectra are reported in pictorial format, rather than in numeric form (see Supporting Information).

Abbreviations used: AcOH, acetic acid; aq., aqueous; Burgess reagent, methyl *N*-(triethylammoniumsulfonyl)carbamate; DCM, dichloromethane; DIPEA, diisopropylethylamine; DMCD, trans-*N,N*-dimethylcyclohexane-1,2-diamine; DMF, dimethylformamide; DMSO, dimethylsulfoxide; EtOAc, ethyl acetate; HCl, hydrochloric acid; FC, flash chromatography; H₂O, water; hex., hexane; hept., heptane; HPLC, high performance liquid chromatography; inorg., inorganic; MeCN, acetonitrile; MeOH, methanol; min, minutes; NaHCO₃, sodium bicarbonate; NaOH, sodium hydroxide; org. organic; prep., preparative; PyBOP, benzotriazol-1-yl-oxy-tris-pyrrolidino-phosphonium-hexafluoro-phosphate; reaction; rt, room temperature; sat., saturated; TBTU, 2-(1*H*-benzotriazole-1-yl)-1,2,3,3-

FULL PAPER

tetramethyluronium tetrafluoroborate; THF, tetrahydrofuran; t_R , retention time.

((R)-3-Hydroxy-piperidin-1-yl)-(5-methyl-2-[1,2,3]triazol-2-yl-phenyl)-methanone (54). TBTU (13.1 g, 40.8 mmol) was added to a rt solution of the **53a**^[31] (7.50 g, 36.9 mmol) and DIPEA (16.3 mL, 95.3 mmol) in DCM (85 mL) and after stirring for 30 min, commercially available (R)-3-hydroxypiperidine HCl **52** (5.08 g, 36.9 mmol) was added. The reaction mixture was stirred at rt for 3 h, then the mixture was washed with water and the inorg. layer extracted with DCM. The combined org. layers were dried (MgSO₄), filtered, concentrated, and the residue was purified on a Biotage (EtOAc/hex. 1:1 to 4:1, R_f = 0.28 (100% EtOAc) yielding **54** (10.3 g, 97%) as a white foam. LC-MS A: t_R = 0.64 min; $[M+H]^+$ = 287.24.

[(R)-3-(5-Chloro-benzooxazol-2-yloxy)-piperidin-1-yl]-(5-methyl-2-[1,2,3]triazol-2-yl-phenyl)-methanone (4). NaH (47 mg, 1.16 mmol) was added to a 0 °C solution of **54** (225 mg, 0.73 mmol) in THF (3.6 mL) and the suspension was stirred at rt for 30 min before 2,5-dichlorobenzo[d]oxazole was added and the resulting mixture stirred for 18 h. The reaction mixture was quenched with water, the inorg. solvent was removed in vacuo and the residue was extracted with DCM (2x). The combined org. layers were dried (MgSO₄), filtered and concentrated. The product was purified by prep. HPLC (Method E) to obtain **4** (7.8 mg) as a white solid. LC-MS A: t_R = 1.01 min; $[M+H]^+$ = 438.01; LC-HRMS: t_R = 1.15 min; $[M+Na]/z$ = 460.1152, found = 460.1160.

(3-Chloro-phenyl)-carbamic acid (R)-1-(5-methyl-2-[1,2,3]triazol-2-yl-benzoyl)-piperidin-3-yl ester (5). NaH (366 mg, 8.38 mmol) was added to a 0 °C solution of **54** (1.29 g, 4.19 mmol) in THF (23 mL) and the resulting mixture was stirred at rt for 20 min, before 3-chlorophenyl isocyanate (1.02 mL, 8.38 mmol) was added and stirred at rt for 2.5 h. The reaction was quenched with sat. aq. NH₄Cl-solution and the product extracted with EtOAc. The inorg. layer was acidified (1 N HCl) and the product was extracted with EtOAc. The combined org. layers were washed with brine, dried (MgSO₄), filtered, and concentrated. Purification by prep. HPLC (Method F) yielded **5** (1.5 g, 60%) as a white solid. LC-MS A: t_R = 0.90 min; $[M+H]^+$ = 440.45; LC-HRMS: t_R = 1.09 min; $[M+H]/z$ = 440.1484, found = 440.1499.

[(R)-3-[3-(3-Chloro-phenyl)-[1,2,4]oxadiazol-5-yl]-piperidin-1-yl]-(5-methyl-2-[1,2,3]triazol-2-yl-phenyl)-methanone (8)

Step 1. **(R)-1-(5-methyl-2-[1,2,3]triazol-2-yl-benzoyl)-piperidine-3-carboxylic acid ethyl ester (56).** TBTU (13.1 g, 40.8 mmol) was added to a rt solution of **53a** (7.50 g, 36.9 mmol) and DIPEA (16.3 mL, 95.3 mmol) in DCM (85 mL), after stirring for 30 min methyl (R)-piperidine-3-carboxylate HCl (**55**) was added (5.8 g, 36.9 mmol) and the resulting mixture was stirred at rt overnight. The reaction mixture was washed with water, the inorg. layer was extracted with DCM and the combined org. layers were dried (MgSO₄), filtered, and concentrated. The product was purified by Biotage (EtOAc/hex. 3:7, R_f = 0.23) yielding **56** (12.14 g, 96%) as a white foam.

Step 2. **(R)-1-(5-methyl-2-[1,2,3]triazol-2-yl-benzoyl)-piperidine-3-carboxylic acid (57).** 2 N aq. NaOH solution (12.5 mL, 25 mmol) was added at rt to a suspension of **56** (6.48 g, 18.9 mmol) in EtOH (20 mL) and THF (20 mL) and the mixture was stirred at rt for 1.5 h. The mixture was concentrated to remove the

organic solvents, then acidified to pH 4 with aq. 1 N HCl and extracted with EtOAc (4x). The combined org. layers were dried (MgSO₄), filtered and concentrated to yield **57** (4.33 g, 73%) as a white solid.

Step 3. PyBOP (249 mg, 0.48 mmol) was added to a 0 °C solution of **57** (100 mg, 0.32 mmol) and DIPEA (0.163 mL, 0.95 mmol) in DCM (2.5 mL). The reaction mixture was stirred at 0 °C for 20 min, then N-hydroxy-3-chloro-benzamidine (60 mg, 0.35 mmol) was added and stirred for 20 min at 0 °C before the reaction mixture was allowed to reach rt overnight. The mixture was quenched with water and extracted with DCM (2x), the combined org. layers were dried (MgSO₄), filtered, and concentrated. To the crude was added dioxane (5 mL) and the reaction mixture was stirred at 90 °C overnight. The mixture was concentrated *in vacuo* and the crude oil was purified by prep. HPLC (Method F) to obtain **8** (6.2 mg, 14%) as a yellowish solid. LC-MS A: t_R = 0.98 min; $[M+H]^+$ = 449.00; LC-HRMS: t_R = 1.23 min; $[M+H]/z$ = 449.1487, found = 449.1500.

N-Ethyl-5-methyl-N-[2-(3-phenyl-[1,2,4]oxadiazol-5-yl)-ethyl]-2-[1,2,3]triazol-2-yl-benzamide (13).

NaBH₄ (15.3 mg, 0.41 mmol) was added to a rt solution of commercially available 2-(3-phenyl-[1,2,4]oxadiazol-5-yl)-ethylamine **62** (61 mg, 0.27 mmol), acetaldehyde (0.015 mL, 0.27 mmol), and TEA (0.08 mL, 0.54 mmol) in MeOH (2 mL) and stirred at rt for 18 h. The reaction mixture was quenched with H₂O and the org. solvent was removed *in vacuo*. The residue was taken up in H₂O and DCM, the org. layer separated and the inorg. layer extracted with DCM (2x). The combined org. layers were dried (MgSO₄), filtered, and concentrated. The crude containing product and remaining starting material was used as such in the next step. TBTU (86.8 mg, 0.27 mmol) was added to a rt solution of the crude **53** (45.8 mg, 0.23 mmol) and DIPEA (0.12 mL, 0.68 mmol) in DMF (2 mL) and the mixture was stirred at rt overnight. Purification by prep. HPLC (Method F) yielded **13** (31 mg, 34%) as a white solid and also **14** (15 mg, 18%, as a side product) was isolated as a white solid. LC-MS B: t_R = 0.87 min; $[M+H]^+$ = 403.09; LC-HRMS: t_R = 1.11 min; $[M+H]/z$ = 403.1877, found = 403.1883.

5-Methyl-N-[2-(3-phenyl-[1,2,4]oxadiazol-5-yl)-ethyl]-2-[1,2,3]triazol-2-yl-benzamide (14). The title compound was isolated as a side product from **13**. LC-MS C: t_R = 0.84 min; $[M+H]^+$ = 375.02; LC-HRMS: t_R = 0.95 min; $[M+H]/z$ = 375.1564, found = 375.1574.

N-Cyclopropylmethyl-5-methyl-N-(3-phenyl-[1,2,4]oxadiazol-5-ylmethyl)-2-[1,2,3]triazol-2-yl-benzamide (15)

Step 1. **Cyclopropylmethyl-(3-phenyl-[1,2,4]oxadiazol-5-ylmethyl)-amine (64)** was synthesized using procedure described for **13**, using commercially available (3-phenyl-1,2,4-oxadiazol-5-yl)methylamine **63** and cyclopropanecarboxaldehyde, yielding **64** (60%) as a yellow oil. LC-MS B: t_R = 0.47 min; $[M+H]^+$ = 230.18. ¹H NMR (400 MHz, CDCl₃) δ : 8.11 (m, 2 H), 7.51 (m, 3 H), 4.18 (s, 2 H), 2.62 (d, J = 6.9 Hz, 2 H), 1.00 (m, 1 H), 0.54 (m, 2 H), 0.18 (m, 2 H).

Step 2. Amid coupling as described for compound **13**, using **64** and **53a** to yield **15** (69%) as a yellowish oil. LC-MS B: t_R = 0.93 min; $[M+H]^+$ = 414.94; LC-HRMS: t_R = 1.18 min; $[M+H]/z$ = 415.1877, found = 415.1886.

FULL PAPER

(5-Methyl-2-[1,2,3]triazol-2-yl-phenyl)-[(S)-2-(3-phenyl-[1,2,4]oxadiazol-5-yl)-pyrrolidin-1-yl]-methanone (19)

Step 1. **(S)-1-(5-Methyl-2-[1,2,3]triazol-2-yl-benzoyl)-pyrrolidine-2-carboxylic acid methyl ester (63)**. TBTU (7.11 g, 22.1 mmol) was added to a rt solution of **53a** (3.00 g, 14.8 mmol) and DIPEA (10.1 mL, 59.1 mmol) in DCM (30 mL), after stirring for 10 min L-proline methylester HCl (**62**) (3.19 g, 15.4 mmol) was added and stirred at rt overnight. The reaction mixture was washed with water, the inorg. layer was extracted with DCM and the combined org. layers were dried (MgSO₄), filtered and concentrated. The product was purified by FC (EtOAc/hept. 7:3) yielding **63** (4.36 g, 94%) as a white solid. LC-MS A: t_R = 0.74 min; [M+H]⁺ = 315.12.

Step 2. **(S)-1-(5-Methyl-2-[1,2,3]triazol-2-yl-benzoyl)-pyrrolidine-2-carboxylic acid (64)**. 2 N aq. NaOH solution (6.3 mL, 12.6 mmol) was added at rt to a suspension of **63** (2.2 g, 7 mmol) in MeOH (9 mL) and THF (9 mL) and the mixture was stirred at rt for 1.5 h. The mixture was concentrated to remove the org. solvents. The residue was acidified to pH 4 with aq. 1 N HCl and extracted with EtOAc (4x). The combined org. layers were dried (MgSO₄), filtered and concentrated to yield **64** (2.0 g, 100%) as a white solid. LC-MS B: t_R = 0.57 min; [M+H]⁺ = 301.03.

Step 3. PyBOP (260 mg, 0.50 mmol) was added to a rt solution of **64** (100 mg, 0.32 mmol) and DIPEA (0.17 mL, 1.00 mmol) in DCM (3 mL), the reaction mixture was stirred for another 10 min, then *N*-hydroxy-benzimidine (**58a**) (60 mg, 0.35 mmol) was added and the mixture was stirred at rt overnight. The mixture was quenched with H₂O and extracted with DCM (2x). The combined org. layers were dried (MgSO₄), filtered, and concentrated. To the crude was added dioxane (4 mL) and the reaction mixture was stirred at 90 °C for 48 h. The mixture was concentrated and purification by prep. HPLC (Method E) yielded **19** (54 mg, 41%) as a beige solid. LC-MS A: t_R = 0.96 min; [M+H]⁺ = 415.25; LC-HRMS: t_R = 1.10 min; [M+H]/z = 401.1721, found = 401.1729.

Compound **36** to **44** were synthesized in analogy to the procedures described for compound **41**.

(5-Methoxy-4-methyl-2-[1,2,3]triazol-2-yl-phenyl)-[(S)-2-[3-(2-trifluoromethoxy-phenyl)-[1,2,4]oxadiazol-5-yl]-pyrrolidin-1-yl]-methanone (41)

Step 1. **2-Bromo-5-methoxy-4-methyl-benzoic acid (69)**. Br₂ (0.79 mL, 15.3 mmol) was added to a rt suspension of 3-methoxy-4-methylbenzoic acid (**68**) (2.12 g, 12.7 mmol) in AcOH (25 mL) and H₂O (25 mL), and the reaction mixture was stirred at 60 °C for 2 h. The mixture was allowed to reach rt and the product which crashed out as a white solid was filtered off and rinsed with cold water to yield **69** (2.81 g, 90%) as a white solid which was used as such in the next step. ¹H NMR (400 MHz, DMSO) δ: 13.30 (s, 1 H), 7.50 (d, J = 0.6 Hz, 1 H), 7.29 (s, 1 H), 3.83 (s, 3 H), 2.18 (s, 3 H).

Step 2. **5-Methoxy-4-methyl-2-[1,2,3]triazol-2-yl-benzoic acid (53b)**. CuI (130 mg, 0.68 mmol) was added in portions to a rt solution of **69** (2.81 g, 11.5 g), 1*H*-1,2,3-triazole (1 mL, 17.3 mmol), DMCDA (0.3 mL, 1.85 mmol). and Cs₂CO₃ (7.47 g, 22.9 mmol) in DMF (20.0 mL) were added and the resulting blue suspension was stirred at 120 °C for 1 h. The mixture was allowed to reach rt, then EtOAc and H₂O was added. The org. layer was separated and the aq. layer was acidified with aq. HCl (24%). The brown-greenish solution was extracted with EtOAc (2x), then the

combined org. extracts were dried (MgSO₄), filtered, and concentrated. Purification and separation of the two isomers were obtained by Biotage (EtOAc/hex. + 0.1 % AcOH 1:9 to 1:1; R_f of product = 0.64 and R_f of undesired isomer = 0.24 in EtOAc (+ 0.1 % AcOH). The product **53b** was isolated as a beige solid (2.15 g, 80%). ¹H NMR (400 MHz, DMSO) δ: 12.96 (s, 1 H), 8.01 (s, 2 H), 7.51 (s, 1 H), 7.28 (s, 1 H), 3.92 (s, 3 H), 2.26 (s, 3 H).

Step 3. **(S)-2-[3-(2-Trifluoromethoxy-phenyl)-[1,2,4]oxadiazol-5-yl]-pyrrolidine-1-carboxylic acid *tert*-butyl ester (66)**. PyBOP (33.41 g, 64.1 mmol) was added to a rt solution of commercially available (*tert*-butoxycarbonyl)-L-proline **65** (11.49 g, 53.4 mmol, and *N*-hydroxy-2-(trifluoromethoxy) benzimidamide **58b** (12.78 g, 53.4 mmol) and DIPEA (27.4 mL, 160 mmol) in DCM (250 mL) and the mixture was stirred at rt for 1 h. The reaction mixture was diluted with DCM and water, the org. layer was separated and the inorg. layer was extracted with DCM. The combined org. layers were washed with brine, dried (MgSO₄), filtered, and concentrated. To the residue was added dioxane (300 mL) and the mixture was stirred at 90 °C for 18 h. The reaction mixture was concentrated, the residue dissolved in EtOAc and washed with aq. sat NaHCO₃ (3x), dried (MgSO₄), filtered, and concentrated. Purification by Biotage (EtOAc/hex. 1:9 to 3:7, R_f = 0.64 EtOAc/hept. 1:1) yielded **66** (13.34 g, 63%) as a yellow oil. LC-MS A: t_R = 0.98 min; [M+H]⁺ = 400.08.

Step 4. **5-(S)-Pyrrolidin-2-yl-3-(2-trifluoromethoxy-phenyl)-[1,2,4]oxadiazole (67)**. TFA (32.1 mL, 419 mmol) was added to a 0 °C solution of **66** in DCM (150 mL) and the mixture was stirred at rt for 5 h. The mixture was concentrated, and the residue dissolved in DCM, and basified with 1 N aq. NaOH until pH 12. The layers were separated and the inorg. layer was extracted with DCM (2x). The combined org. layers were dried (MgSO₄), filtered, and concentrated to yield **67** (9.4 g, 94%) as a yellow oil which was used as such in the next step. ¹H NMR (400 MHz, DMSO) δ: 8.07-8.11 (m, 1 H), 7.69-7.76 (m, 1 H), 7.59-7.66 (m, 2 H), 4.57 (dd, J₁ = 5.2 Hz, J₂ = 8.3 Hz, 1 H), 2.88-2.99 (m, 2 H), 2.19 (m, 1 H), 1.99-2.08 (m, 1 H), 1.71-1.92 (m, 2 H). LC-MS A: t_R = 0.62 min; [M+H]⁺ = 300.12.

Step 5. TBTU (2.64 g, 8.23 mmol) was added to a rt solution of **53b** (1.6 g, 6.86 mmol) and DIPEA (3.5 mL, 20.6 mmol) in DCM (20 mL), after stirring for 15 min a solution of **67** (2.05 g, 6.86 mmol) in DCM (10.0 mL) was added and the resulting mixture was stirred at rt for 1 h. The reaction mixture was washed with sat. aq. NaHCO₃ and the org. layer was dried (MgSO₄), filtered and concentrated. The product was purified by Biotage (EtOAc/hex. 1:9 to 3:7, R_f = 0.30 in EtOAc/hept. 1:1) yielding **41** (2.7 g, 77%) as a white foam. LC-MS A: t_R = 1.01 min; [M+H]⁺ = 515.10; LC-HRMS: t_R = 1.22 min; [M+H]/z = 515.1650, found = 515.1665.

(5-Methoxy-4-methyl-2-[1,2,3]triazol-2-yl-phenyl)-[(S)-2-[5-(2-trifluoromethoxy-phenyl)-[1,2,4]oxadiazol-3-yl]-pyrrolidin-1-yl]-methanone (51)

Step 1. **(S)-2-(*N*-Hydroxycarbamimidoyl)-pyrrolidine-1-carboxylic acid *tert*-butyl ester (71)**. Hydroxylamine HCl (1.70 g, 24.2 mmol) was added to a rt solution of commercially available (S)-1-boc-2-cyanopyrrolidine (**70**) (3.0 g, 15.3 mmol) and Na₂CO₃ (1.98 g, 23.6 mmol) in MeOH (30 mL) and the resulting suspension was stirred at 70 °C for 1 h. The reaction mixture was filtered, the filter cake washed with MeOH and the filtrate concentrated. The residue was dissolved in EtOAc and H₂O, the org. layer separated and the inorg. layer extracted with EtOAc

FULL PAPER

(1x). The combined org. layers were dried (MgSO_4), filtered and concentrated to yield 3.2 g of **71** (91%) as a white solid, which was used as such in the next step. LC-MS A: t_R = 0.45 min; $[\text{M}+\text{H}]^+$ = 230.23.

Step 2. **(S)-2-[5-(2-Trifluoromethoxy-phenyl)-[1,2,4]oxadiazol-3-yl]-pyrrolidine-1-carboxylic acid tert-butyl ester (73a)**. TBTU (10.02 g, 31.2 mmol) was added to a rt solution of 2-(trifluoromethoxy)benzoic acid (**72a**) (5.10 g, 24 mmol) and DIPEA (10.3 mL, 60 mmol) in DCM (50 mL). The resulting reaction mixture was stirred at rt for 10 min, then **71** (7.93 g, 32.2 mmol) was added and stirring was continued for 1.5 h at rt. The reaction mixture was concentrated and to the residue was added dioxane (30 mL) and the reaction-mixture was stirred at 80 °C for 2 days. The reaction mixture was concentrated, DCM was added, and the org. layer was washed with aq. sat. NaHCO_3 solution. The org. layer was dried (MgSO_4), filtered, and concentrated. Purification by Biotage (EtOAc/hex. 1:9 to 3:7; R_f = 0.38 in EtOAc/hept. 3:7) yielded **73a** (8.27 g, 86%) as a yellow oil. LC-MS A: t_R = 0.99 min; $[\text{M}+\text{H}]^+$ = 400.12.

Step 3. **3-(S)-Pyrrolidin-2-yl-5-(2-trifluoromethoxy-phenyl)-[1,2,4]oxadiazole (74a)**. TFA (16 mL, 209 mmol) was added to a rt solution of **73a** (8.27 g, 20.7 mmol) in DCM (100 mL) and the resulting mixture was stirred at rt for 1.5 h. The reaction mixture was concentrated (to remove the excess TFA) and the residue was dissolved in DCM and aq. 4 N NaOH solution was added until pH 12. The layers were separated, and the aq. layer was extracted with DCM (1x). The comb. org. layers were dried (MgSO_4), filtered, and concentrated to yield **74a** (5.45 g, 90%) as a yellowish oil, which was used as such in the next step. LC-MS A: t_R = 0.63 min; $[\text{M}+\text{H}]^+$ = 300.12.

Step 4. TBTU (4.47 g, 13.9 mmol) was added to a rt solution of **53b** (2.50 g, 10.7 mmol) and DIPEA (4.59 mL, 26.8 mmol) in DCM (20 mL) and the reaction mixture was stirred for 20 min at this temperature before **74a** (3.53 g, 11.8 mmol) dissolved in DCM (5 mL) was added and the resulting mixture was stirred at rt for 70 min. The reaction mixture was diluted with DCM and water. The layers were separated, and the org. layer was dried (MgSO_4), filtered, and concentrated. Purification by FC (EtOAc/hept. 1:1) yielded **51** (4.89 g, 89%) as a white solid. LC-MS A: t_R = 1.0 min; $[\text{M}+\text{H}]^+$ = 515.12; LC-HRMS: t_R = 1.21 min; $[\text{M}+\text{H}]/z$ = 515.1650, found = 515.1662.

(5-Methyl-2-[1,2,3]triazol-2-yl-phenyl)-((S)-2-[5-(2-trifluoromethoxy-phenyl)-[1,3,4]oxadiazol-2-yl]-pyrrolidin-1-yl)-methanone (46)

Step 1. **(S)-2-[5-(2-Trifluoromethoxy-phenyl)-[1,3,4]oxadiazol-2-yl]-pyrrolidine-1-carboxylic acid tert-butyl ester (77a)**. PyBOP (520 mg, 1.00 mmol) was added to a 0 °C solution of Boc-L-proline (200 mg, 0.67 mmol), 2-(trifluoromethoxy)benzoic acid hydrazide **76a** (91 mg, 0.67 mmol) and DIPEA (0.37 mL, 2.13 mmol) in DCM (25 mL) and the reaction mixture was stirred at rt overnight. The reaction mixture was washed with sat. aq. NaHCO_3 and the inorg. layer was re-extracted with DCM. The combined org. layers were, dried (MgSO_4), filtered, and concentrated. The residue was dissolved in dioxane (8 mL) and Burgess reagent (1.85 g, 7.77 mmol) was added. The resulting reaction mixture was irradiated in the microwave for 30 min at 110 °C (without cooling). The reaction mixture was diluted with a sat. NaHCO_3 solution, extracted with EtOAc (2x) and the combined org. layers were dried (MgSO_4), filtered, and

concentrated. The product was purified by Biotage (EtOAc/hex. 1:9 to 3:7; R_f = 0.25 in EtOAc/hept. 1:1) yielding **77a** (840 mg, 81% over 2 steps) as a white foam.

Step 2. **(S)-2-[5-(2-Trifluoromethoxy-phenyl)-[1,3,4]oxadiazol-2-yl]-pyrrolidine-1-carboxylic acid tert-butyl ester (78a)**. TFA (2 mL, 26.1 mmol) was added to a rt solution of **77a** (840 mg, 2.1 mmol) in DCM (5.0 mL) and the reaction mixture was stirred at rt overnight. The reaction mixture was concentrated, and the residue taken up in DCM, then basified with 4 N aq. NaOH. The org. layer was separated and the inorg. layer extracted with DCM. The combined org. layers were dried (MgSO_4), filtered, and concentrated to yield **78** (quantitatively) as a yellow oil. ^1H NMR (400 MHz, DMSO) δ : 9.82-10.14 (m, 1 H), 8.16 (dd, J_1 = 1.9 Hz, J_2 = 8.3 Hz, 1 H), 7.82-7.94 (m, 1 H), 7.65-7.75 (m, 2 H), 5.18 (t, J = 7.7 Hz, 1 H), 3.40 (m, 2 H), 2.45-2.57 (m, 1 H), 2.37 (m, 1 H), 2.03-2.21 (m, 2 H).

Step 3. TBTU (50.1 mg, 0.16 mmol) was added to a rt solution of **53a** (24.3 mg, 0.12 mmol), DIPEA (61 μL , 0.36 mmol) in DMF (0.5 mL) and after stirring for 10 min at rt, a solution of **78a** (27.5 mg, 0.12 mmol) in DMF (0.5 mL) was added and the reaction mixture was stirred at rt overnight. Purification by prep. HPLC (Method F) yielded **46** (32 mg, 58%) as a slightly yellow solid. LC-MS A: t_R = 0.93 min; $[\text{M}+\text{H}]^+$ = 485.06; LC-HRMS: t_R = 1.08 min; $[\text{M}+\text{H}]/z$ = 485.1544, found = 485.1551.

Acknowledgements

The authors gratefully thank Stephanie Bazire, Jeanine Thanner, Markus Gude, Celia Müller-Grandjean, Katalin Menyhart, Thomas Sasse, Cedric Fischer, Stephane Delahaye, Isabelle Weber, Fabienne Drouet, Eric Soubieux, Rolf Wuest, Julia Khobzaoui and Sandrine Chopinet.

Keywords: drug design • dual orexin receptor antagonists • insomnia • sleep disorder • structure-activity relationship

References:

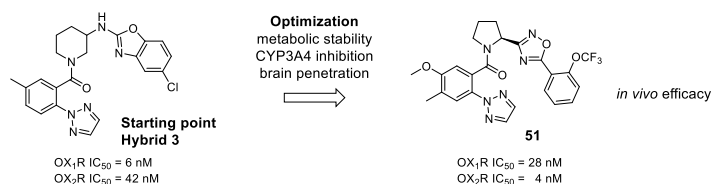
- [1] L. Citrome, *Int. J. Clin. Pract.* **2014**, *68*, 1429-1441.
- [2] A. K. Dubey, S. S. Handu, P. K. Mediratta, *J. Pharmacol. Pharmacother.* **2015**, *6*, 118-121.
- [3] C. D. Cox, J. J. Renger, P. J. Coleman, C. J. Winrow, *Med. Chem. Rev.* **2015**, *50*, 419-432.
- [4] C. Brisbare-Roch, J. Dingemans, R. Koberstein, P. Hoefer, H. Aissaoui, S. Flores, C. Mueller, O. Nayler, J. van Gerven, S. L. de Haas, P. Hess, C. Qiu, S. Buchmann, M. Scherz, T. Weller, W. Fischli, M. Clozel, F. Jenck, *Nat. Med.* **2007**, *13*, 150-155.
- [5] L. De Lecea, T. S. Kilduff, C. Peyron, X. Gao, P. E. Foye, P. E. Danielson, C. Fukuhara, E. L. Battenberg, V. T. Gautvik, F. S. Bartlett, 2nd, W. N. Frankel, A. N. van den Pol, F. E. Bloom, K. M. Gautvik, J. G. Sutcliffe, *Proc. Natl. Acad. Sci. U. S. A.* **1998**, *95*, 322-327.
- [6] T. Sakurai, A. Amemiya, M. Ishii, I. Matsuzaki, R. M. Chemelli, H. Tanaka, S. C. Williams, J. A. Richardson, G. P. Kozlowski, S. Wilson, J. R. Arch, R. E. Buckingham, A. C. Haynes, S. A. Carr, R. S. Annan, D. E. McNulty, W. S. Liu, J. A. Terrett, N. A. Elshourbagy, D. J. Bergsma, M. Yanagisawa, *Cell* **1998**, *92*, 573-585.
- [7] C. Boss, C. Roch, *Bioorg. Med. Chem. Lett.* **2015**, *25*, 2875-2887.
- [8] A. J. Roecker, C. D. Cox, P. J. Coleman, *J. Med. Chem.* **2016**, *59*, 504-530.

FULL PAPER

- [9] S. P. Andrews, S. J. Aves, J. A. Christopher, R. Nonoo, *Curr. Top. Med. Chem.* **2016**, *16*, 3438-3469.
- [10] K. Janto, J. R. Prichard, S. Pusalavidyasagar, *J. Clin. Sleep Med.* **2018**, *14*, 1399-1408.
- [11] W. J. Herring, T. Roth, A. D. Krystal, D. Michelson, *J. Sleep Res.* **2019**, *28*, e12782.
- [12] P. Hoever, G. Dorffner, H. Benes, T. Penzel, H. Danker-Hopfe, M. J. Barbanjo, G. Pillar, B. Saletu, O. Polo, D. Kunz, J. Zeitlhofer, S. Berg, M. Partinen, C. L. Bassetti, B. Hogl, I. O. Ebrahim, E. Holsboer-Trachsler, H. Bengtsson, Y. Peker, U. M. Hemminger, E. Chiossi, G. Hajak, J. Dingemanse, *Clin. Pharmacol. Ther.* **2012**, *91*, 975-985.
- [13] D. N. Neubauer, *Curr. Opin. Investig. Drugs* **2010**, *11*, 101-110.
- [14] Y. Yoshida, Y. Naoe, T. Terauchi, F. Ozaki, T. Doko, A. Takemura, T. Tanaka, K. Sorimachi, C. T. Beuckmann, M. Suzuki, T. Ueno, S. Ozaki, M. Yonaga, *J. Med. Chem.* **2015**, *58*, 4648-4664.
<https://clinicaltrials.gov/ct2/show/NCT02919319>.
- [15] *Press Release Minerva Bioscience:*
www.minervaneurosciences.com: "Minerva Neuroscience Reports Positive Phase 1 Data with MIN-202, Selective Orexin-2 Antagonist for Treatment of Sleep Disorders Including Primary and Comorbid Insomnia" **2015**.
- [16] *Press Release Minerva Bioscience:*
www.minervaneurosciences.com: "Minerva Neuroscience Announces Enrollment of First Patient in Phase 2b Trial of Seltorexant (MIN-202) in Patients With Insomnia Disorder" **2017**.
- [17] A. J. Roecker, T. S. Reger, M. C. Mattern, S. P. Mercer, J. M. Bergman, J. D. Schreier, R. V. Cube, C. D. Cox, D. Li, W. Lemaire, J. G. Bruno, C. M. Harrell, S. L. Garson, A. L. Gotter, S. V. Fox, J. Stevens, P. L. Tannenbaum, T. Prueksaritanont, T. D. Cabalu, D. Cui, J. Stellabott, G. D. Hartman, S. D. Young, C. J. Winrow, J. J. Renger, P. J. Coleman, *Bioorg. Med. Chem. Lett.* **2014**, *24*, 4884-4890.
- [18] A. J. Roecker, S. P. Mercer, J. D. Schreier, C. D. Cox, M. E. Fraley, J. T. Steen, W. Lemaire, J. G. Bruno, C. M. Harrell, S. L. Garson, A. L. Gotter, S. V. Fox, J. Stevens, P. L. Tannenbaum, T. Prueksaritanont, T. D. Cabalu, D. Cui, J. Stellabott, G. D. Hartman, S. D. Young, C. J. Winrow, J. J. Renger, P. J. Coleman, *ChemMedChem* **2014**, *9*, 311-322.
- [19] C. Betschart, S. Hintermann, D. Behnke, S. Cotesta, M. Fendt, C. E. Gee, L. H. Jacobson, G. Laue, S. Ofner, V. Chaudhari, S. Badiger, C. Pandit, J. Wagner, D. Hoyer, *J. Med. Chem.* **2013**, *56*, 7590-7607.
- [20] A. Kumar, P. Chanana, S. Choudhary, *Pharmacological Reports* **2016**, *68*, 231-242.
- [21] C. Dugovic, J. E. Shelton, L. E. Aluisio, I. C. Fraser, X. Jiang, S. W. Sutton, P. Bonaventure, S. Yun, X. Li, B. Lord, C. A. Dvorak, N. I. Carruthers, T. W. Lovenberg, *J. Pharmacol. Exp. Ther.* **2009**, *330*, 142-151.
- [22] A. Gozzi, G. Turrini, L. Piccoli, M. Massagrande, D. Amantini, M. Antolini, P. Martinelli, N. Cesari, D. Montanari, M. Tessari, M. Corsi, A. Bifone, *PLoS one* **2011**, *6*, 16406.
- [23] P. Bonaventure, J. Shelton, S. Yun, D. Nepomuceno, S. Sutton, L. Aluisio, I. Fraser, B. Lord, J. Shoblock, N. Welty, S. R. Chaplan, Z. Aguilar, R. Halter, A. Ndifor, T. Koudriakova, M. Rizzolio, M. Letavic, N. I. Carruthers, T. Lovenberg, C. Dugovic, *J. Pharmacol. Exp. Ther.* **2015**, *354*, 471-482.
- [24] S. D. Kuduk, J. W. Skudlarek, C. N. Di Marco, J. G. Bruno, M. A. Pausch, J. A. O'Brien, T. D. Cabalu, J. Stevens, J. Brunner, P. L. Tannenbaum, A. L. Gotter, C. J. Winrow, J. J. Renger, P. J. Coleman, *Bioorg. Med. Chem. Lett.* **2014**, *24*, 1784-1789.
- [25] M. Mieda, E. Hasegawa, Y. Y. Kisanuki, C. M. Sinton, M. Yanagisawa, T. Sakurai, *J. Neurosci.* **2011**, *31*, 6518-6526.
- [26] A. L. Gotter, M. S. Forman, C. M. Harrell, J. Stevens, V. Svetnik, K. L. Yee, X. Li, A. J. Roecker, S. V. Fox, P. L. Tannenbaum, S. L. Garson, I. D. Lepeleire, N. Calder, L. Rosen, A. Struyk, P. J. Coleman, W. J. Herring, J. J. Renger, C. J. Winrow, *Sci. Rep.* **2016**, *6*, 27147.
- [27] P. L. Johnson, W. Truitt, S. D. Fitz, P. E. Minick, A. Dietrich, S. Sanghani, L. Traskman-Bendz, A. W. Goddard, L. Brundin, A. Shekhar, *Nat. Med.* **2010**, *16*, 111-115.
- [28] E. Merlo Pich, S. Melotto, *Front. Neurosci.* **2014**, *8*, 26.
- [29] H. Knust, M. Nettekoven, E. Pinard, O. Roche, M. Rogers-Evans, Hoffmann-La Roche, Inc., USA . 2009
- [30] C. D. Cox, M. J. Breslin, D. B. Whitman, J. D. Schreier, G. B. McGaughey, M. J. Bogusky, A. J. Roecker, S. P. Mercer, R. A. Bednar, W. Lemaire, J. G. Bruno, D. R. Reiss, C. M. Harrell, K. L. Murphy, S. L. Garson, S. M. Doran, T. Prueksaritanont, W. B. Anderson, C. Tang, S. Roller, T. D. Cabalu, D. Cui, G. D. Hartman, S. D. Young, K. S. Koblan, C. J. Winrow, J. J. Renger, P. J. Coleman, *J. Med. Chem.* **2010**, *53*, 5320-5332.
- [31] C. D. Cox, P. J. Coleman, M. J. Breslin, I. T. Raheem, J. D. Schreier, A. J. Roecker, Merck Sharp & Dohme Corp., USA . WO2010048012A1, **2010**
- [32] S. D. Kuduk, J. W. Skudlarek, C. N. DiMarco, J. G. Bruno, M. H. Pausch, J. A. O'Brien, T. D. Cabalu, J. Stevens, J. Brunner, P. L. Tannenbaum, S. L. Garson, A. T. Savitz, C. M. Harrell, A. L. Gotter, C. J. Winrow, J. J. Renger, P. J. Coleman, *Bioorg. Med. Chem. Lett.* **2015**, *25*, 2488-2492.
- [33] D. C. Beshore, S. D. Kuduk, N. Liverton, Y. Luo, N. Meng, T. Yu, Merck Sharp & Dohme Corp., USA . 2015
- [34] N. Liverton, D. C. Beshore, S. D. Kuduk, Y. Luo, N. Meng, T. Yu, Merck Sharp & Dohme Corp., USA . 2015
- [35] B. Heidmann, J. Gatfield, C. Roch, A. Treiber, S. Tortoioli, C. Brotschi, J. T. Williams, M. H. Bolli, S. Abele, T. Sifferlen, F. Jenck, C. Boss, *ChemMedChem* **2016**.
- [36] J. Boström, A. Hogner, A. Llinàs, E. Wellner, A. T. Plowright, *J. Med. Chem.* **2012**, *55*, 1817-1830.
- [37] S. Nordhoff, S. Bulat, S. Cerezo-Gálvez, O. Hill, B. Hoffmann-Enger, M. López-Canet, C. Rosenbaum, C. Rummey, M. Thiemann, V. G. Matassa, P. J. Edwards, A. Feurer, *Bioorg. Med. Chem. Lett.* **2009**, *19*, 6340-6345.
- [38] C. J. Winrow, A. L. Gotter, C. D. Cox, P. L. Tannenbaum, S. L. Garson, S. M. Doran, M. J. Breslin, J. D. Schreier, S. V. Fox, C. M. Harrell, J. Stevens, D. R. Reiss, D. Cui, P. J. Coleman, J. J. Renger, *Neuropharmacology* **2012**, *62*, 978-987.
- [39] T. Sifferlen, C. Boss, E. Cottreel, R. Koberstein, M. Gude, H. Aissaoui, T. Weller, J. Gatfield, C. Brisbare-Roch, F. Jenck, *Bioorg. Med. Chem. Lett.* **2010**, *20*, 1539-1542.
- [40] H. Aissaoui, R. Koberstein, C. Zumbunn, J. Gatfield, C. Brisbare-Roch, F. Jenck, A. Treiber, C. Boss, *Bioorg. Med. Chem. Lett.* **2008**, *18*, 5729-5733.
- [41] C. Boss, C. Brisbare-Roch, F. Jenck, H. Aissaoui, R. Koberstein, T. Sifferlen, T. Weller, *Chimia* **2008**, *62*, 974-979.
- [42] T. Sifferlen, R. Koberstein, E. Cottreel, A. Boller, T. Weller, J. Gatfield, C. Brisbare-Roch, F. Jenck, C. Boss, *Bioorg. Med. Chem. Lett.* **2013**, *23*, 3857-3863.
- [43] C. Boss, C. Roch-Brisbare, M. A. Steiner, A. Treiber, H. Dietrich, F. Jenck, M. von Raumer, T. Sifferlen, C. Brotschi, B. Heidmann, J. T. Williams, H. Aissaoui, R. Siegrist, J. Gatfield, *ChemMedChem* **2014**.
- [44] T. Sifferlen, A. Boller, A. Chardonneau, E. Cottreel, J. Gatfield, A. Treiber, C. Roch, F. Jenck, H. Aissaoui, J. T. Williams, C. Brotschi, B. Heidmann, R. Siegrist, C. Boss, *Bioorg. Med. Chem. Lett.* **2015**, *25*, 1884-1891.
- [45] M. Bolli, C. Boss, C. Brotschi, M. Gude, B. Heidmann, T. Sifferlen, J. T. Williams, Actelion Pharmaceuticals Ltd., Switz. WO2014057435A1, **2014**
- [46]

FULL PAPER

Entry for the Table of Contents



The orexin system plays an important role in the regulation of wakefulness. Herein, we outline our optimization efforts towards a novel dual orexin receptor antagonist (DORA). Our starting point was compound **3**, a hybrid of Merck's suvorexant and another published DORA containing a piperidine as a core structure. Our work led to the identification of compound **51**, a potent, brain penetrating DORA with *in vivo* efficacy comparable to suvorexant in the rat.